Journal of Computational Mathematics, Vol.18, No.5, 2000, 467–480.

ON THE EXPLICIT COMPACT SCHEMES II: EXTENSION OF THE STCE/CE METHOD ON NONSTAGGERED GRIDS*[1)]

Hua-zhong Tang and Hua-mu Wu
(*State Key Laboratory of Scientific and Engineering Computing, Institute of Computational Mathematics, Chinese Academy of Sciences, Beijing 100080, China*)

Abstract

This paper continues to construct and study the explicit compact (EC) schemes for conservation laws. First, we extend STCE/SE method on non-staggered grid, which has same well resolution as one in [1], and just requires half of the computational works. Then, we consider some constructions of the EC schemes for two-dimensional conservation laws, and some 1D and 2D numerical experiments are also given.

Key words: Conservation laws, Compact scheme, Shock–capturing method, Euler equations.

1. Introduction

This paper is interested in the genuinely nonlinear conservation laws

$$\frac{\partial u}{\partial t} + \sum_{i=1}^{d} \frac{\partial f^i(u)}{\partial x^i} = 0, \tag{1.1}$$

with initial data $u(0,x) = u_0(x),\ x = (x^1, ..., x^d)$.

It is well known that the above problem may not always have a smooth global solution even if the initial data u_0 is adequately smooth[6]. Thus, we consider its weak solution so that the problem (1.1) might have a global solution allowing discontinuities(e.g. shock wave etc.). Moreover, the entropy condition should be imposed in order to single out a physically relevant solution(also called the entropy solution)[5, 6, 7].

In the last two decades, there has been an enormous amount of activity related to the construction and analysis of finite difference methods which approximate nonlinear hyperbolic equation (or system) of conservation laws, and are expected to have:

* Received March 17, 1997.

[1)] This work was supported in part by National Natural Science Foundation of China, the State Major Key Project for Basic Research, and Laboratory of Computational Mathematics of Beijing Institute of Applied Physics and Computational Mathematics.

(1) limit solutions which satisfy a entropy condition.

(2) the absence of spurious oscillations in the approximate solutions.

(3) at least second-order accuracy in region of smoothness, except for certain isolated points, or lines, or surfaces.

Some of the earliest work in the design of schemes having properties (2) and (3) above was done by van Leer[15], Harten[3, 4] and Sweby[10]. However, property (1) seems difficulty to prove for high-order finite difference schemes[11, 12, 17]. Here we are concerned with properties (2) and (3).

Recently Chang in [1] presented a new numerical method for 1D conservation laws, referred to as the method of space-time conservation element and solution element (STCE/SE), from a new framework. This framework differs substantially in both concept and methodology from the well-established methods e.g. finite difference, finite volume, finite element and spectral methods. But, based on his framework, it seems difficulty to be extended for multi-dimensional conservation laws.

The aim of this paper is to construct and study the explicit compact (EC) method for conservation laws based on Chang's STCE/SE framework. The paper is organized as follows. In section 2 we extend STCE/SE method to non-staggered grid for 1D conservation laws. The results show that our schemes have the same well resolution as one in [1], and just require half of computational works. In section 3 we consider construction of two classes of the EC schemes for 2D conservation laws. In section 4 some numerical experiments are given. The problems include interaction of blast waves, interaction of a moving Mach=3 shock with sine waves and regular shock reflection etc.

2. The Explicit Compact Methods for 1D Conservation Laws

Consider 1D conservation laws

$$\frac{\partial u}{\partial t} + \frac{\partial f(u)}{\partial x} = 0, \tag{2.1}$$

with initial data $u(0, x) = u_0(x)$.

As in [1], let $\xi_1 = x$, $\xi_2 = t$ be considered as the coordinates of a two dimensional Euclidean space E_2. Let Ω denote the set of mesh points (j, n) in E_2, where $n, j = 0, \pm 1, \pm 2, \cdots$, respectively. Let Ω_1 and Ω_2 denote respectively the two subsets of Ω, which are defined by

$$\Omega_1 = \{(j, n) \mid j + n \text{ is even}\}, \quad \Omega_2 = \{(j, n) \mid j + n \text{ is odd}\}.$$

Then for each $(j, n) \in \Omega_k (k = 1 \; or \; 2)$, there is a *solution element* $(SE_k(j, n))$ associated

with each $(j,n) \in \Omega_k$, which is taken as

$$SE_k(j,n) = \{(\xi_1,\xi_2) \mid x_{j-1} < \xi_1 < x_{j+1}, \xi_2 = t^n\} \cup \{(\xi_1,\xi_2) \mid t^{n-1} < \xi_2 < t^{n+1}, \xi_1 = x_j\}, \quad \forall (j,n) \in \Omega_k. \tag{2.2}$$

Again, E_2 can also be covered by uniform nonoverlapping rectangular regions referred to as *conservation element* ($CE_k(j,n)$) associated with each $(j,n) \in \Omega_k$, which is defined by

$$CE_k(j,n) = \{(\xi_1,\xi_2) \mid x_{j-1} < \xi_1 < x_{j+1}, t^{n-1} < \xi_2 < t^n\}, \quad \forall (j,n) \in \Omega_k. \tag{2.3}$$

Note that the Euclidean space E_2 will be covered by two sets of the uniform nonoverlapping SEs and two sets of the uniform nonoverlapping CEs, respectively, according to the above definitions of solution element and conservation element.

Using Gauss' divergence theorem in the space-time E_2, we have the following integral form of the conservation laws (2.1)

$$\oint_{\partial V} \vec{h} \cdot d\vec{s} = 0, \quad \vec{h} = (f(u), u), \tag{2.4}$$

where (1) ∂V is the boundary of an arbitrary space-time region V in E_2; (2) $\vec{h}$ is a current density vector in E_2; and (3) $d\vec{s} = \vec{n} d\sigma$ with $d\sigma$ and $\vec{n}$, respectively, being the area and the outward unit normal of a surface element on ∂V. Note that $\vec{h} \cdot d\vec{s}$ is the space-time flux of $\vec{h}$ leaving the region V through the surface element $d\vec{s}$ on ∂V.

For any $(x,t) \in SE_k(j,n)$, $u(x,t)$, $f(x,t)$, and $\vec{h}$ are approximated respectively by $u^*(x,t;j,n)$, $f^*(x,t;j,n)$ and $\vec{h}^*(x,t;j,n)$, which are defined as

$$\begin{aligned} u^*(x,t;j,n) &= u_j^n + (u_x)_j^n (x - x_j) + (u_t)_j^n (t - t^n), \\ f^*(x,t;j,n) &= f_j^n + (f_x)_j^n (x - x_j) + (f_t)_j^n (t - t^n), \\ \vec{h}^*(x,t;j,n) &= (f^*(x,t;j,n), u^*(x,t;j,n)). \end{aligned} \tag{2.5}$$

Now, if let $V = CE_k(j,n)$, then equation (2.4) can be approximated by

$$\oint_{\partial(CE_k(j,n))} \vec{h}^* \cdot d\vec{s} = 0. \tag{2.6}$$

By a simple calculation, we can derive the following explicit compact scheme:

Algorithm(ECS-I):

$$u_j^n = \frac{u_{j-1}^{n-1} + u_{j+1}^{n-1}}{2} - \frac{\Delta t}{2\Delta x}(f_{j+1}^{n-1} - f_{j-1}^{n-1}) + \frac{\Delta x}{4}[(u_x)_{j-1}^{n-1} - (u_x)_{j+1}^{n-1}] - \frac{\Delta t^2}{4\Delta x}[(f_t)_{j+1}^{n-1} - (f_t)_{j-1}^{n-1}]. \tag{2.7}$$

On the other hand, the scheme solving $(u_x)_j^n$ can be given as

$$(u_x)_j^n = W_0((u_x^-)_j^n, (u_x^+)_j^n; \alpha), \tag{2.8}$$

where

$$W_0(a, b; \alpha) = \begin{cases} \dfrac{\mid a \mid^\alpha b + \mid b \mid^\alpha a}{\mid a \mid^\alpha + \mid b \mid^\alpha}, & \text{if } \mid a \mid + \mid b \mid > 0 \\ 0, \quad \text{otherwise} \end{cases} \tag{2.9}$$

and

$$(u_x^\pm)_j^n = \pm\frac{1}{\Delta x}[u_{j\pm1}^{n-1} + \Delta t(u_t)_{j\pm1}^{n-1} - u_j^n]. \tag{2.10}$$

Remark. (1) The explicit compact scheme (2.7)–(2.10) is of second order accuracy in space and time, and can be easily extended to 1D system of conservation laws. We refer the readers to [1] for details. (2) In order to obtain higher order accurate schemes, we can use higher order Taylor expansion to replace ones in (2.5) to approximate $u(x,t)$, $f(x,t)$, and $\vec{h}$, respectively. (3) The scheme (2.7)–(2.10) is of compact stencil, because it is a explicit two-level three-point finite difference scheme in the conservative form.

3. The Explicit Compact Methods for 2D Conservation Laws

This section considers 2D conservation laws

$$\frac{\partial u}{\partial t} + \frac{\partial f(u)}{\partial x} + \frac{\partial g(u)}{\partial y} = 0, \tag{3.1}$$

with initial data $u(0, x, y) = u_0(x, y)$.

Similarly, if let $\xi_1 = x$, $\xi_2 = y$, $\xi_3 = t$ be considered as the coordinates of a three-dimensional Euclidean space E_3, and Ω denote the set of mesh points (j, k, n) in E_3, where $n, j, k = 0, \pm1, \cdots$, respectively, then we can give two kinds of *solution element*(SE) and *conservation element* (CE) associated with each $(j, k, n) \in \Omega$ as follows:
Method A Let $\Omega_i (i = 1, 2, 3, 4)$ denote the four subsets of Ω, respectively, defined as

$$\begin{aligned} \Omega_1 &= \{(j,k,n) \mid j+n \text{ is even}, \quad k+n \text{ is even}\}; \\ \Omega_2 &= \{(j,k,n) \mid j+n \text{ is odd}, \quad k+n \text{ is odd}\}; \\ \Omega_3 &= \{(j,k,n) \mid j+n \text{ is even}, \quad k+n \text{ is odd}\}; \\ \Omega_4 &= \{(j,k,n) \mid j+n \text{ is odd}, \quad k+n \text{ is even}\}. \end{aligned}$$

Then for each $(j,k,n) \in \Omega_i (i = 1\ or\ 2\ or\ 3\ or\ 4)$, there is a *solution element* $(SE_i(j,k,n))$ and a *conservation element* $(CE_i(j,k,n))$ associated with each grid point $(j,k,n) \in \Omega_i$ which are defined by

$$\begin{aligned} SE_i(j,k,n) = &\{(\xi_1,\xi_2,\xi_3) \mid x_{j-1} < \xi_1 < x_{j+1}, y_{k-1} < \xi_2 < y_{k+1}, \xi_3 = t^n\} \\ &\cup\{(\xi_1,\xi_2,\xi_3) \mid t^{n-1} < \xi_3 < t^{n+1}, y_{k-1} < \xi_2 < y_{k+1}, \xi_1 = x_j\} \\ &\cup\{(\xi_1,\xi_2,\xi_3) \mid t^{n-1} < \xi_3 < t^{n+1}, x_{j-1} < \xi_1 < x_{j+1}, \xi_2 = y_k\}, \end{aligned} \tag{3.2}$$

and

$$\begin{aligned} CE(j,k,n) = \{(\xi_1,\xi_2,\xi_3) \mid &x_{j-1} < \xi_1 < x_{j+1}, y_{k-1} < \xi_2 < y_{k+1}, \\ &t_{n-1} < \xi_3 < t_n\}, \end{aligned} \tag{3.3}$$

for all $(j,k,n) \in \Omega_i$.

Method B Similarly, define the two subsets $\Omega_i (i = 1,2)$ of Ω as

$$\begin{aligned} \Omega_1 &= \{(j,k,n) \mid j+k+n \text{ is even}\}; \\ \Omega_2 &= \{(j,k,n) \mid j+k+n \text{ is odd}\}. \end{aligned}$$

For the sake of simplicity in the presentation, let A^l, B^l, C^l, D^l, and O^l represent the mesh point (x_{j-1}, y_k, t^l), (x_j, y_{k-1}, t^l), (x_{j+1}, y_k, t^l), (x_j, y_{k+1}, t^l) and (x_j, y_k, t^l), respectively, where $l = n\ or\ n-1$. let M^l_{AB}, M^l_{BC}, M^l_{CD}, and M^l_{DA} represent the midpoint of the line A^lB^l, B^lC^l, C^lD^l, and D^lA^l, $(l = n$ or $l = n-1)$, respectively. Then *solution element* $(SE_i(j,k,n))$ and *conservation element* $(CE_i(j,k,n))$ associated with each grid point $(j,k,n) \in \Omega_i$ can be defined as

$$\begin{aligned} SE_i(j,k,n) = &\{\text{the interior region of quadrilateral } A^nB^nC^nD^n\} \\ &\cup\{\text{the interior region of quadrilateral } M^n_{AB}M^n_{CD}M^{n-1}_{CD}M^{n-1}_{AB}\} \\ &\cup\{\text{the interior region of quadrilateral } M^n_{AD}M^n_{BC}M^{n-1}_{CB}M^{n-1}_{DA}\}, \end{aligned} \tag{3.4}$$

and

$$\begin{aligned} CE_i(j,k,n) = \{&\text{the union of the interior of hexahedron} \\ &A^nB^nC^nD^n - A^{n-1}B^{n-1}C^{n-1}D^{n-1} \text{ and its boundary}\}. \end{aligned} \tag{3.5}$$

By using Gauss' divergence theorem in the space-time E_3, we have the following integral version of conservation laws (3.1)

$$\oint_{\partial V} \vec{h} \cdot d\vec{s} = 0, \quad \vec{h} = (f(u), g(u), u), \tag{3.6}$$

where (1) ∂V is the boundary of an arbitrary space-time region V in E_3; (2) $\vec{h}$ is a current density vector in E_3; and (3) $d\vec{s} = d\sigma\vec{n}$ with $d\sigma$ and $\vec{n}$, respectively, being the

area and the outward unit normal of a surface element on ∂V. Note that $\vec{h}\cdot d\vec{s}$ is the space-time flux of $\vec{h}$ leaving the region V through the surface element $d\vec{s}$ on ∂V.

For any $(x,y,t)\in SE_i(j,k,n)$, we approximate $u(x,y,t)$, $f(x,y,t)$, $g(x,y,t)$, and $\vec{h}$, by $u^*(x,y,t;j,k,n)$, $f^*(x,y,t;j,k,n)$, $g^*(x,y,t;j,k,n)$, and $\vec{h}^*(x,y,t;j,k,n)$, respectively, which are defined as

$$\begin{aligned}
u^*(x,y,t;j,k,n) &= u^n_{j,k}+(u_x)^n_{j,k}(x-x_j)+(u_y)^n_{j,k}(y-y_k)+(u_t)^n_{j,k}(t-t^n),\\
f^*(x,y,t;j,k,n) &= f^n_{j,k}+(f_x)^n_{j,k}(x-x_j)+(f_y)^n_{j,k}(y-y_k)+(f_t)^n_{j,k}(t-t^n),\\
g^*(x,y,t;j,k,n) &= g^n_{j,k}+(g_x)^n_{j,k}(x-x_j)+(g_y)^n_{j,k}(y-y_k)+(g_t)^n_{j,k}(t-t^n),\\
\vec{h}^*(x,y,t;j,k,n) &= (f^*(x,y,t;j,k,n),g^*(x,y,t;j,k,n),u^*(x,y,t;j,k,n)).
\end{aligned} \tag{3.7}$$

Similarly, if let $V=CE_i(j,k,n)$ defined in *Method A (i=1 or 2 or 3 or 4)*, or *Method B (i=1 or 2)* , then equation (3.6) can be approximated by

$$\oint_{\partial(CE_i(j,k,n)}\vec{h}^*\cdot d\vec{s}=0. \tag{3.8}$$

Corresponding to two definitions of $SE_i(j,k,n)$ and $CE_i(j,k,n)$, we can derive two kinds of the explicit compact methods for 2D conservation laws, respectively.
Algorithm(ECS-II):

$$\begin{aligned}
u^{n+1}_{j,k} = \frac{1}{4}\,(\,&u^n_{j+1,k+1}+u^n_{j+1,k-1}+u^n_{j-1,k+1}+u^n_{j-1,k-1}\,)\\
&+\frac{\Delta x}{8}[(u_x)^n_{j-1,k-1}-(u_x)^n_{j+1,k-1}+(u_x)^n_{j-1,k+1}-(u_x)^n_{j+1,k+1}]\\
&+\frac{\Delta y}{8}[(u_y)^n_{j-1,k-1}+(u_y)^n_{j+1,k-1}-(u_y)^n_{j-1,k+1}-(u_y)^n_{j+1,k+1}]\\
&-\frac{\Delta t}{4\Delta x}\,[F^n_{j+1,k+1}+F^n_{j+1,k-1}-F^n_{j-1,k+1}-F^n_{j-1,k-1}]\\
&-\frac{\Delta t}{4\Delta y}\,[G^n_{j+1,k+1}+G^n_{j-1,k+1}-G^n_{j+1,k-1}-G^n_{j-1,k-1}]\\
&+\frac{\Delta t\Delta y}{8\Delta x}[(f_y)^n_{j+1,k+1}-(f_y)^n_{j-1,k+1}-(f_y)^n_{j+1,k-1}+(f_y)^n_{j-1,k-1}]\\
&+\frac{\Delta t\Delta x}{8\Delta y}[(g_x)^n_{j+1,k+1}-(g_x)^n_{j-1,k+1}-(g_x)^n_{j+1,k-1}+(g_x)^n_{j-1,k-1}],
\end{aligned} \tag{3.9}$$

where $F=f+\frac{\Delta t}{2}(f_t)$ and $G=g+\frac{\Delta t}{2}(g_t)$.
Algorithm(ECS-III):

$$\begin{aligned}
u^{n+1}_{j,k} = \frac{1}{4}\,(\,&u^n_{j+1,k}+u^n_{j,k-1}+u^n_{j-1,k}+u^n_{j,k+1})+\frac{\Delta x}{8}[(u_x)^n_{j-1,k}-(u_x)^n_{j+1,k}]\\
&+\frac{\Delta y}{8}[(u_y)^n_{j,k-1}-(u_y)^n_{j,k+1}]-\frac{\Delta t}{2\Delta x}[F^n_{j+1,k}-F^n_{j-1,k}]-\frac{\Delta t}{2\Delta y}[G^n_{j,k+1}-G^n_{j,k-1}].
\end{aligned} \tag{3.10}$$

The scheme solving $(u_x)_j^n$ can be given in a similar way

$$\begin{aligned}(u_x)_{j,k}^n &= W_0((u_x^-)_{j,k}^n, (u_x^+)_{j,k}^n; \alpha),\\ (u_y)_{j,k}^n &= W_0((u_y^-)_{j,k}^n, (u_y^+)_{j,k}^n; \alpha),\end{aligned} \tag{3.11}$$

where $W_0(a, b; \alpha)$ is defined in (2.9), and

$$\begin{aligned}(u_x^{\pm})_{j,k}^n &= \pm\frac{1}{\Delta x}[u_{j\pm1,k}^{n-1} + \Delta t(u_t)_{j\pm1,k}^{n-1} - u_{j,k}^n],\\ (u_y^{\pm})_{j,k}^n &= \pm\frac{1}{\Delta y}[u_{j,k\pm1}^{n-1} + \Delta t(u_t)_{j,k\pm1}^{n-1} - u_{j,k}^n].\end{aligned} \tag{3.12}$$

Remark. (1) The above schemes (3.7)–(3.12) are of second order accuracy in space and time, and can also be extended conveniently to 2D system of conservation laws. (2) In order to obtain higher order accurate schemes, we can use higher order Taylor expansion to approximate $u(x, y, t)$, $f(x, y, t)$, and $\vec{h}$ etc., respectively. (3) The above schemes are also of compact stencil, because they are explicit two-level five-point finite difference scheme in conservative form.

4. Numerical Results

In this section we present some numerical experiments to demonstrate the performance of the above three explicit compact schemes, which includes resolution and entropy-valiging.

Consider Euler equations

$$\frac{\partial U}{\partial t} + \frac{\partial F(U)}{\partial x} + \frac{\partial G(U)}{\partial y} = 0, \tag{4.1}$$

where

$$U = \begin{pmatrix}\rho\\ \rho u\\ \rho v\\ E\end{pmatrix},\ F(U) = \begin{pmatrix}\rho u\\ \rho u^2 + p\\ \rho uv\\ u(E+p)\end{pmatrix},\ G(U) = \begin{pmatrix}\rho v\\ \rho uv\\ \rho v^2 + p\\ v(E+p)\end{pmatrix},$$

with

$$p = (\gamma - 1)\left(E - \frac{1}{2}\rho(u^2 + v^2)\right).$$

Here ρ, u, v, p and E denote the gas density, velocity, pressure, and total energy, respectively, $m = \rho u, n = \rho v$ is the momentum and we take $\gamma = 1.4$.

4.1 1D Problem

Example 1. The first problem considered is the Lax shock tube problem[3]. The set of data is

$$U_L = \begin{pmatrix} 0.445 \\ 0.311 \\ 8.928 \end{pmatrix}, \; U_R = \begin{pmatrix} 0.5 \\ 0 \\ 1.4275 \end{pmatrix}. \tag{4.2}$$

The numerical results at $t = 0.16$ shown in Fig.1, are obtained by the ECS-I method with 200 points under the CFL restriction with CFL= 0.95. The exact solution is shown by the solid lines.

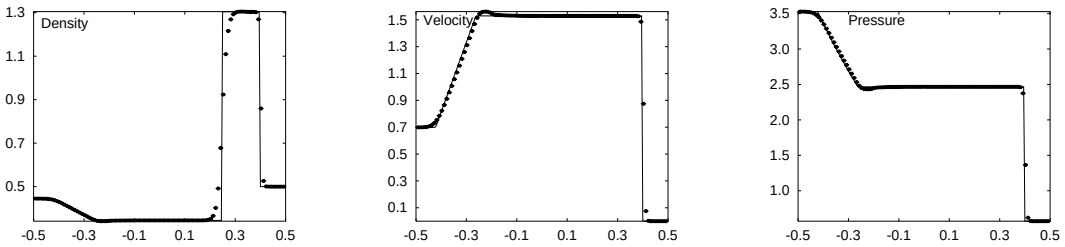

Fig.1. The Lax's shock tube problem (4.2), CFL=0.95, $t = 0.16$.

Example 2. The second problem is the Sod shock tube problem with initial data

$$U_L = \begin{pmatrix} 1.0 \\ 0.0 \\ 2.5 \end{pmatrix}, \; U_R = \begin{pmatrix} 0.125 \\ 0.0 \\ 0.25 \end{pmatrix}. \tag{4.3}$$

The numerical results at $t = 0.20$ shown in Fig.2, are obtained by the ECS-I method with 200 points. The exact solution is shown by the solid lines. Our results can be comparable to the results obtained by the STCE/SE method presented in [1].

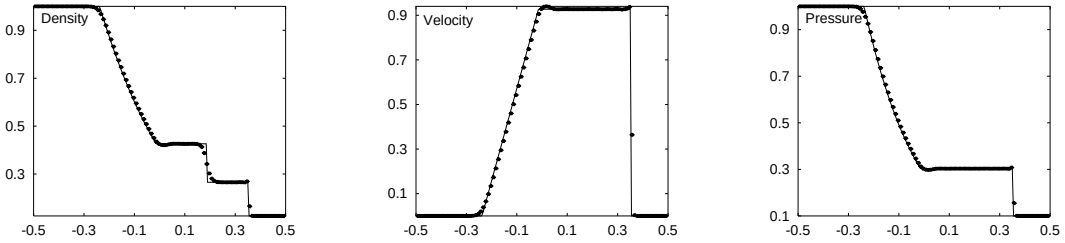

Fig.2. The Sod's shock tube problem (4.3), CFL=0.95, t=0.2.

Example 3. The next problems is the stationary shock problems with Mach=10.0 and 4.0, respectively, and the stationary expansion shock problem with Mach=4.0[3].

To further examine the entropy-validing and the resolution of the scheme, we consider now a Riemann problem where the two states, say U_1 and U_2, satisfy the Rankine-Hugoniot relations in the direction of the field $u - c$, with a zero speed of proagation. Fixing the state U_1 by assigning values to ρ_1, p_1, and the Mach number $M_1 = u_1/c_1$, the state v_2 is determined by

$$\begin{aligned} p_2/p_1 &= (2\gamma M_1^2 - \gamma + 1)/(\gamma + 1), \\ u_2/u_1 &= (2\gamma M_1^2 + \gamma - 1)/(\gamma + 1), \\ \rho_2/\rho_1 &= u_1/u_2. \end{aligned} \tag{4.4}$$

In Figs.3–5 we test the scheme on stationary shock with $W_L = U_1$ and $W_R = U_2$. First we set $\rho_1 = p_1 = 1,\ M_1 = 4$ (which gives $p_2/p_1 = 18.5$) and test the scheme for resolution. The results are shown in Fig.3. In Fig.4 we further test the STCE/SE method for robustness by applying it to a very strong shock $\rho_1 = p_1 = 1,\ M_1 = 10$ with a pressure ratio of $p_2/p_1 = 116.5$.

In Fig.5, for entropy-validing the scheme is applyed to the inadmissible "stationary" discontinuity $W_L = U_2$ and $W_R = U_1$ with $\rho_1 = p_1 = 1,\ M_1 = 4 and 10$ It has been shown in [3] that a nonphysical phenomenon can be formed by applying some TVD schemes to this problem. From Figs.3–5 we observe that the stationary shocks are resolved very well, but there are only slight numerical overshoots or oscillations at the both sides; the stationary expansion shock problem is also resolved very well.

The calculations in Figs.3–5 were performed at $t = 0.2$ under the CFL restriction CFL= 0.95 with 200 cells.

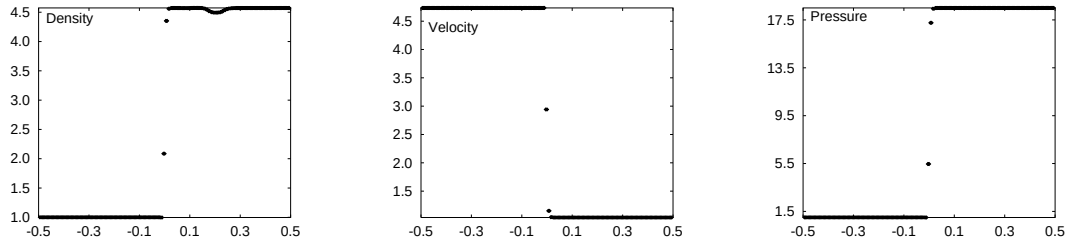

Fig.3. The stationary shock problem, CFL=0.95, Mach=4, t=0.2.

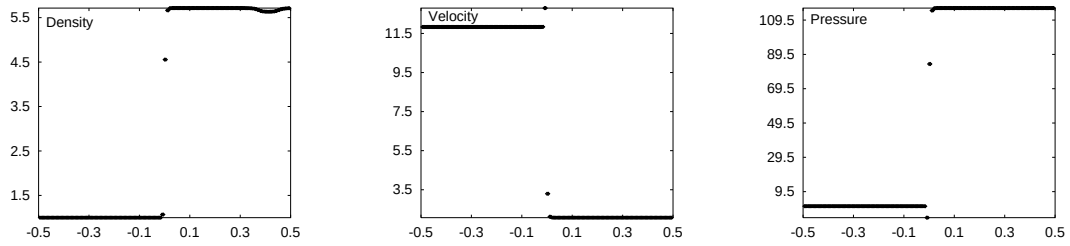

Fig.4. The stationary shock problem, CFL=0.95, Mach=10, t=0.2.

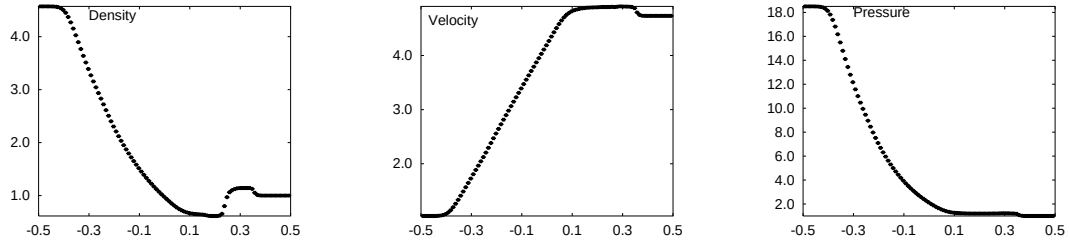

Fig.5. The stationary expansion shock, CFL=0.95, Mach=4, t=0.2.

Example 4. The next problem is interaction of a moving Mach=3 shock with sine waves in density[9]. The initial data is given as follows

$$\rho_L = 3.857143,\ m_L = 2.629369,\ p_L = 10.33333 \text{ when } x < -4,$$

$$\rho_R = 1 + \epsilon \sin(5x),\ m_R = 0,\ p_R = 1 \text{ when } x \geq -4.$$

If $\epsilon = 0$, this is a pure Mach=3 shock moving to the right. Here We take $\epsilon = 0.2$. For a linearized analysis of this problem see [8].

In Fig.6, the dashed lines and solid lines are numerical solution with 400 points and 2000 points, respectively, sames as the resolutions in [9].

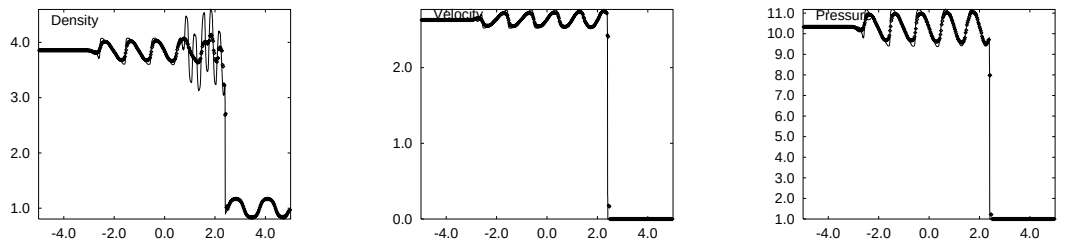

Fig.6. Interaction of a moving $Mach = 3$ shock with sine waves, CFL=0.95, t=1.8

Example 5. Here we present numerical experiments with the ECS-I method for

the interaction of Blast Waves[4, 16] with initial data

$$U(x,0) = \begin{cases} U_L, & 0 \leq x < 0.1, \\ U_M, & 0.1 \leq x < 0.9, \\ U_R, & 0.9 \leq x < 1, \end{cases} \tag{4.5}$$

where

$$\rho_L = \rho_M = \rho_R = 1,\ u_L = u_M = u_R = 0,\ p_L = 1000,\ p_M = 0.01,\ p_R = 100.$$

The boundaries at $x = 0$ and $x = 1$ are solid walls. This problem was suggested by Woodward and Colella[16] as a test problem;

In our calculations we divided the interval (0, 1) into N cells by

$$x_j = (j - \frac{1}{2})/N,\ j = 1, ..., N,$$

where x_j marks the center of the jth cell. The boundary conditions of a solid wall in $x = 0$ and $x = 1$ were treated by reflection[4].

In Fig.7 we show the solution of the ECS-I method at $t = 0.038$, respectively, with CFL= 0.95. The dashed lines and solid lines are numerical solution with 800 points and 2000 points, respectively.

The ECS-I method captures important structures on the fine grid and the results are comparable to other high resolution schemes in [4, 16].

We refer the reader to [4, 16], where a comprehensive comparison of the performance of various schemes for this problem is presented, and a highly accurate solution is displayed and a detailed description of the various interactions that occur at these instances is presented.

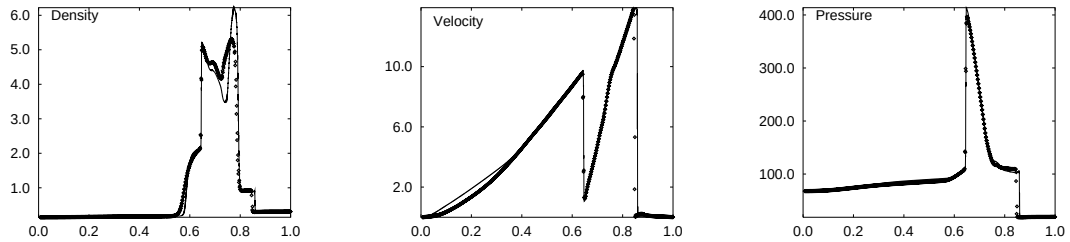

Fig.7. Interaction of blast waves, CFL=0.95, t=0.038.

Example 6. The final 1D problem considered is low density and internal energy

Riemann problem[2] with initial data

$$U(x,0) = \begin{cases} U_L, & 0 \leq x < 0.5, \\ U_R, & 0.5 \leq x \leq 1, \end{cases} \tag{4.6}$$

where

$$\rho_L = \rho_R = 1,\ u_L = -2,\ u_R = 2,\ E_L = E_R = 3.$$

It has been observed that schemes which are based on a linearized Riemann solver (e.g., Roe's scheme) may lead to an unphysical negative density or internal energy during the computational process[2]. The ECS-I method does suffer from negative density when CFL > 0.5. However, The ECS-I method does succeed when CFL < 0.5. In Fig.8, the dotted lines and solid lines are numerical solution with 200 points and 2000 points at $t = 0.15$, respectively.

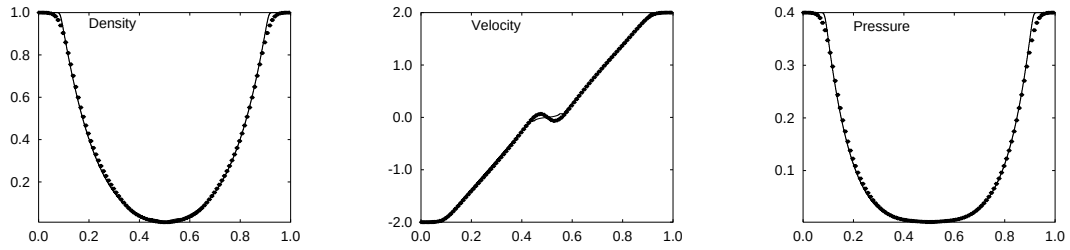

Fig.8. Low density and internal energy Riemann problem, CFL=0.45, t=0.15.

4.2 2D Problems

Example 7. The 2D problem considered is regular shock reflection problem. The computational domain is a rectangle of length 4 and height 1 divided into $M \times N$ rectangular grids with $\Delta x = 1/(M-1)$ and $\Delta y = 1/(N-1)$. Dirichlet conditions are imposed on the left and upper boundaries as

$$(\rho,\ u,\ v, p) =|_{0,y,t}= (1, 2.9, 0, 0.714286),$$

$$(\rho,\ u,\ v, p) =|_{x,1,t}= (1.69997, 2.61934, -0.50633, 1.52919).$$

The bottom boundary is a reflecting wall and the supersonic outflow condition is applied along the right boundary. Initially, the entire flow field is set equal to the free stream supersonic inflow values. Our results obtained by using the ECS-II method and the ECS-III method, respectively, have shown in Figs.9a and 9b, with 15 contours.

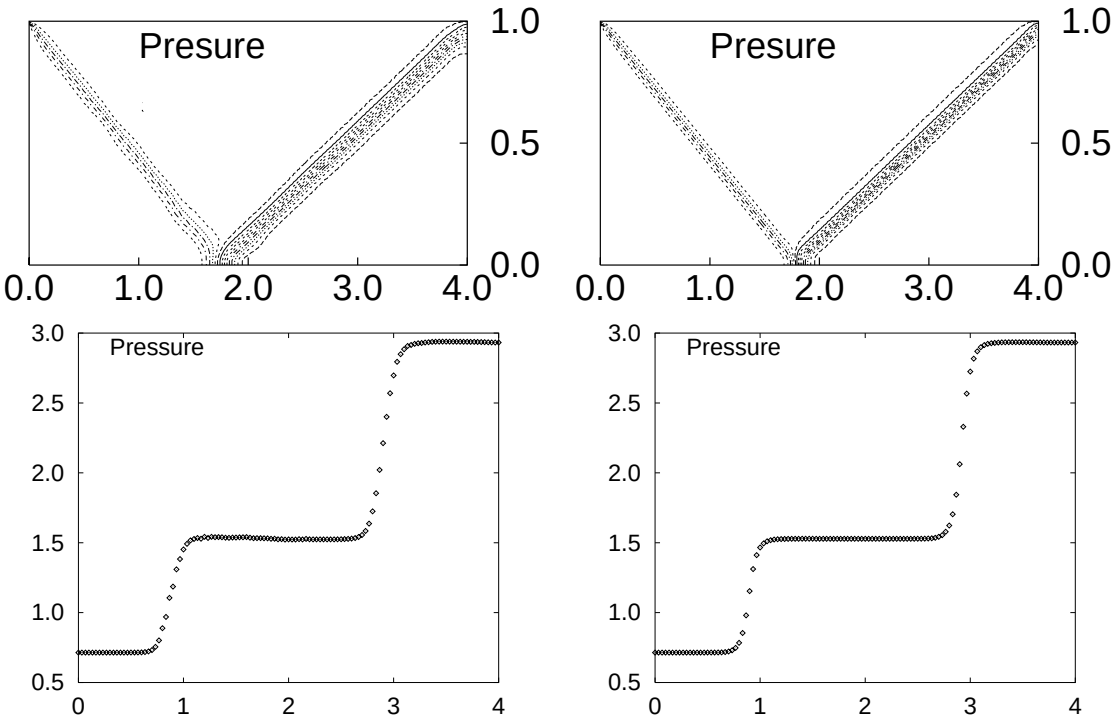

(a). Scheme ECS-II; (b). Scheme ECS-III

Fig.9. Regular shock reflection, 120×60 grids, CFL=0.45.

5. Conclusion

In this paper, we have further studied the EC schemes for conservation laws. A new EC method on non-staggered grid is constructed, which requires half of computational works, and has the same well resolution as in [8]. Moreover two EC schemes for two–dimensional conservation laws are also constructed. Some numerical results have shown current EC schemes are of well resolution and entropy-validing. Unfortunately, we cannot to give the theory of nonlinear stability (e.g. TVB etc.) and entropy condition for the EC methods. In future, we will extend the EC schemes to 3D case and nonuniform grid case, and apply this method to numerical simulations in engineering.

References

[1] S.C. Chung, The method of space-time conservation element and solution element—A new approach for solving the Navier-Stokes and Euler equations, *J. Comput. Phys.,* **119** (1995), 295-324.

[2] B. Einfeldt, C.D. Munz, P.L. Roe, and B. Sjogreen, On Godunov-type methods near low densities, *J. Comput. Phys.,* **92** (1991), 273-295.

[3] A. Harten, High resolution schemes for hyperbolic conservation laws, *J. Comput. Phys.,* **49** (1983), 357-393.

[4] A. Harten, B. Engquist, S. Osher, and S.R. Chakravarthy, Uniformly high order accurate essentially non-oscillatory schemes, III, *J. Comput. Phys.,* **71** (1987), 231–303.

[5] S.N.Kružkov, First order quasilinear equations in several independent variables, *Math. USSR Sbornik,* **10** (1970), 217–243.

[6] P.D. Lax, Hyperbolic systems of conservation laws II, *Comm. Pure Appl. Math.,* **10** (1957), 537–566.

[7] P.D. Lax, Hyperbolic systems of conservation laws and the mathematical theory of shock waves, SIAM, Philadelphia, 1973.

[8] J. McKenzie, K. Westphal, *Phys. Fluids,* **11** (1968), 2350.

[9] C.W. Shu and S. Osher, Efficient implementation of essentially non-oscillatory shock-capturing schemes, II, *J. Comput. Phys.,* **83** (1989), 32–78.

[10] P.K. Sweby, High resolution schemes using flux limiters for hyperbolic conservation laws, *SIAM J. Num. Anal,* **21** (1984), 995–1011.

[11] E. Tadmor, Numerical viscosity and the entropy condition for conservative difference schemes, *Math. Comp.,* **43** (1984), 369–381.

[12] H.Z. Tang and H.M. Wu, On a cell entropy inequality for the relaxing schemes for scalar conservation laws, *J. Comput. Math.,* **18**(2000), 69–74.

[13] H.Z. Tang and H.M. Wu, On the explicit compact schemes I: Numerical experiments on the STCE/SE method for 1D Euler equations, to appear, 1997.

[14] H.Z. Tang and H.M. Wu, On the explicit compact schemes III: Higher order schemes constructed by Taylor series, to appear, 1997.

[15] Van Leer, Towards the ultimate conservative difference schemes. V. A second-order sequel to Godunov's method, *J. Comput. Phys.,* **32** (1979), 101–136.

[16] P.R. Woodward and P. Colella, The numerical simulation of two-dimensional fluid flow with strong shocks, *J. Comput. Phys.,* **54** (1984), 115–173.

[17] N. Zhao and H.Z. Tang, High resolution schemes and discrete entropy conditions for 2-D linear conservation laws, *J. Comput. Math.,* **13** (1995), 281–289.